Research Square

Preprints are preliminary reports that have not undergone peer review.
They should not be considered conclusive, used to inform clinical practice,
or referenced by the media as validated information.

Energy Optimization in a Two-Tier Aerial-Terrestrial Collaborative Edge Computing Network

hossein rahmani
Ghasem Mirjalily
mirjalily@yazd.ac.ir

Jamshid Abouei

Research Article

Keywords: Mobile edge computing, unmanned aerial vehicle, energy efficiency, trajectory planning

Posted Date: November 13th, 2026

DOI: https://doi.org/10.21203/rs.3.rs-11207257/v1

License: This work is licensed under a Creative Commons Attribution 4.0 International License.
Read Full License

Additional Declarations: No competing interests reported.

Energy Optimization in a Two-Tier Aerial-Terrestrial Collaborative Edge Computing Network

Hossein Rahmani, Ghasem Mirjalily, and Jamshid Abouei

Abstract- This paper proposes a two-tier edge computing architecture that integrates multiple UAVs with terrestrial Base Stations (BSs) to provide flexible and energy-efficient computing services. A joint optimization framework is developed to minimize overall energy consumption by jointly optimizing communication and computing resource allocation, task offloading, and the trajectories of multiple UAVs. The resulting formulation is a highly coupled non-convex optimization problem involving computation, communication, mobility, and energy-related variables. To address this complexity, appropriate transformation and convexification techniques are employed to obtain tractable subproblems and iteratively derive an efficient solution. Simulation results demonstrate that the proposed framework can effectively reduce overall energy consumption while maintaining the required network performance, highlighting the potential of UAV-based edge resources to reduce users' energy consumption. Furthermore, the integration of multi-UAVs and Non-Orthogonal Multiple Access (NOMA) improves spectrum utilization and contributes to reducing the overall energy consumption of the proposed network. Unlike acceleration-based fixed-wing formulations, the constant-speed rotary-wing propulsion model adopted here yields a convex propulsion energy and thereby reduces the computational complexity of the trajectory optimization.

Key words: Mobile edge computing, unmanned aerial vehicle, energy efficiency, trajectory planning.

I. INTRODUCTION

The rapid growth of computation-intensive and latency-sensitive applications in next-generation wireless networks has created a strong need for efficient edge computing architectures. Mobile Edge Computing (MEC) addresses this challenge by moving computational resources closer to end users, thereby reducing communication latency and the energy required for task execution and data transmission. However, conventional terrestrial MEC networks may face limitations in coverage, deployment flexibility, and wireless channel conditions, particularly in dense or dynamically changing environments. Unmanned Aerial vehicles (UAVs) have therefore emerged as promising aerial platforms for MEC systems owing to their mobility, flexible deployment, and favorable Line-of-Sight (LoS) communication characteristics [1], [2]. By integrating UAVs with terrestrial MEC infrastructure, aerial edge resources can complement ground-based servers and provide additional computing and communication capabilities [3]. Nevertheless, the limited onboard energy of UAVs and the energy consumption of ground users make efficient resource management a fundamental challenge in UAV-assisted MEC networks [4], [5].

Authors are with the Department of Electrical Engineering, Yazd University, Yazd, Iran
G. Mirjalily (corresponding author), e-mail: mirjalily@yazd.ac.ir

In addition to improving network coverage and flexibility, efficient spectrum utilization is essential for supporting a large number of users while satisfying their communication and computational requirements. According to the Shannon capacity relationship [6], the available bandwidth has a direct impact on the achievable data rate and, consequently, on transmission energy and latency. Non Orthogonal Multiple Access (NOMA) enables multiple users to share the same spectrum resources through power-domain multiplexing, potentially improving spectral efficiency and reducing communication overhead for task offloading [7]. Therefore, integrating NOMA with UAV-assisted MEC can provide an effective means of jointly exploiting aerial mobility and efficient spectrum sharing for energy-aware edge computing. To facilitate the integration of aerial edge resources without requiring fundamental modifications to the existing terrestrial infrastructure, the conventional Orthogonal Multiple Access (OMA)-based mechanism is retained in the Ground Base Station (GBS)-based subnetwork, while NOMA is introduced in the UAV-based subnetwork. In this way, the proposed architecture combines the compatibility of the existing terrestrial network with the enhanced spectrum utilization enabled by NOMA in the newly introduced aerial layer.

Motivated by these considerations, this paper develops an energy-efficient two-tier UAV-assisted MEC framework in which GBSs and multiple UAVs jointly provide edge computing services to Ground Users (GUs). The proposed framework jointly accounts for communication, computation, and UAV mobility. In particular, the trajectories of multiple UAVs are optimized together with resource allocation to exploit favorable wireless channels while accounting for the energy consumed by UAV movement and communication. This joint design establishes a trade-off between improving the communication conditions of users and limiting the energy expenditure associated with UAV operation.

The resulting resource management is formulated as a joint optimization problem involving communication resources, computational resources, task offloading, and multi-UAV trajectories. Due to the strong coupling among these variables and the presence of non-convex constraints, the formulated problem is computationally challenging. To obtain an efficient solution, appropriate transformation and convexification techniques are employed to convert the original problem into a sequence of tractable subproblems, which are solved iteratively.

A summary of representative studies on UAV-assisted MEC networks and a comparison with the proposed framework are presented in Table I. As summarized in Table I, previous studies have investigated various aspects of UAV-assisted MEC, including hybrid aerial-terrestrial architectures, multi-UAV deployment, UAV trajectory optimization, and NOMA-based communication. However, the joint integration of these features under a hybrid access architecture, where OMA is retained for the existing GBS-based subnetwork and NOMA is introduced for the newly deployed UAV-based subnetworks, has received limited attention. This motivates the development of the proposed framework, which aims to exploit aerial edge resources while preserving the existing terrestrial access structure and improving the energy efficiency of the overall MEC network.

Table I. Comparison of representative UAV-assisted MEC studies with the proposed framework.

Ref.	hybrid GBS & UAV Network	Multi-UAV	UAV Trajectory Optimization	Hybrid OMA/NOMA access
[2]	✓	-	✓	-
[8]	-	-	-	-
[9]	-	✓	✓	-
[10]	-	-	✓	-
[11]	-	-	✓	-
[12]	✓	✓	-	-
[13]	-	-	✓	-
[14]	-	✓	✓	-
[15]	✓	✓	-	-
[16]	-	✓	✓	-
[17]	✓	-	✓	-
Proposed Approach	✓	✓	✓	✓

The main contributions of this paper are summarized as follows:

1. **Two-tier hybrid aerial-terrestrial MEC architecture:** We propose a hybrid edge computing architecture consisting of a macro cell with N_{gb} GBSs and N_{uav} UAV subnetworks, where each UAV serves its corresponding subnetwork. The UAV subnetworks are deployed within the coverage region of the macro cell, enabling terrestrial and aerial edge resources to jointly serve GUs.
2. **Joint energy-aware resource optimization:** We formulate a joint optimization problem that considers radio and computational resource allocation, task offloading, and multi-UAV trajectories. The objective is to minimize the overall energy consumption associated with GU computation and communication, UAV operation, and GBS operation.
3. **Multi-UAV trajectory optimization:** The mobility of multiple UAVs is explicitly incorporated into the optimization framework. The UAV trajectories are jointly optimized with resource allocation to exploit favorable channel conditions while accounting for the propulsion energy required for UAV movement.
4. **Hybrid OMA/NOMA access:** We retain OMA for GU–GBS communications while employing NOMA for GU–UAV communications. This design enables the integration of advanced aerial edge resources without requiring fundamental changes to the existing terrestrial access structure.
5. **Efficient solution of the non-convex problem:** The resulting optimization problem is highly non-convex due to the coupling among communication, computation, and UAV mobility variables. Appropriate transformation, convexification, and iterative optimization techniques are employed to obtain a tractable and efficient solution. Simulation results demonstrate the effectiveness of the proposed framework in reducing energy consumption, particularly the energy consumption of GUs, while maintaining the required communication and computing performance.

In this paper, compared with our earlier framework [3], we replace the acceleration-based fixed-wing UAV propulsion model, whose energy consumption is non-convex with respect to the trajectory variables, with a constant-speed rotary-wing model, for which the energy consumption is convex in the UAV displacement. This eliminates an entire class of non-convexity from the trajectory subproblem and reduces the number of SCA stages required by the overall algorithm. Furthermore, the channel model is refined from a single probabilistic LoS/NLoS model at 2 GHz applied to both tiers to a tier-specific model, with a probabilistic LoS/NLoS channel at 5.8 GHz for the UAV tier and a pure NLoS channel at 3.5 GHz for the GBS tier. These changes alter the feasible set, the convexity structure, and the resulting energy trade-offs, and therefore constitute a distinct methodological contribution rather than an incremental extension.

The remainder of this paper is organized as follows. Section II presents the proposed system model and communication channel, followed by the mathematical formulation of the energy minimization problem. Section III presents the proposed solution approach, including UAV trajectory optimization and joint radio and computational resource allocation. Section IV presents the simulation results and evaluates the performance of the proposed framework. Finally, Section V concludes the paper and outlines potential directions for future work. The notation used throughout this paper is summarized in Table II.

TABLE II. LIST OF NOTATIONS

Symbol	Description
$N_{gu} \backslash N_{uav} \backslash N \backslash N_{gb}$	Number of: GUs/UAVs/Time slots/GBSs
$f_{i,m} \backslash f_{i,b}$	Computation capacity of m^{th} UAV /b^{th} GBS allocated to i^{th} GU
f_i	Local computation capacity of i^{th} GU
$d_{i,m} \backslash d_{i,b}$	Number of bits processed by UAV/GBS MEC servers in the network for i^{th} GU
d_i	Number of bits processed locally by i^{th} GU
D_i	Total computing tasks of i^{th} GU
$O_{i,b}[n] \backslash O_{i,m}[n]$	Offloaded bits to b^{th} GBS \m^{th} UAV by i^{th} GU in the n^{th} time slot
$E_{comp}^{USER} \backslash E_{comp}^{UAVs} \backslash E_{comp}^{GBSs}$	Total computing energy consumption of GUs, UAVs and GBSs MEC servers
$p_{i,m} \backslash p_{i,b}$	Transmit power from i^{th} GU to m^{th}/b^{th} MEC server
$w_{user} \backslash w_{gbs} \backslash w_{uav}$	Weight factors associated with GUs, GBSs and UAVs
$E_{comm}^{UAV} \backslash E_{comm}^{GBS}$	Total offloading energy to all UAVs / GBSs in uplink
E_{move}^{UAV}	Total propulsion energy consumption of *M* UAVs in *N* time slots
$\boldsymbol{r}_m$	Instantaneous UAV position
$\boldsymbol{v}_m$	UAV velocity
$g_{i,s}[n]$	Channel gain between i^{th} GU and s^{th}server in n^{th} time slot
γ	UAVs movement weight factor

II. SYSTEM MODEL AND MAIN ASSUMPTIONS

A. Communication Model

We consider the network illustrated in Fig. 1, where the GUs, denoted by $\{i \mid i = 1, \dots, N_{gu}\}$ are uniformly distributed over the considered service area. Each GU has a computational task that must be finished within a given duration of T seconds. Considering the substantially limited processing capability of users, some GBSs, denoted by $\{b \mid b = 1, \dots, N_{gb}\}$, and UAVs denoted by $\{m \mid m = 1, \dots, N_{uav}\}$ are deployed to provide computation capabilities for resource- constrained users. The set of all MEC servers including GBSs and UAVs is denoted by $\{s \mid s = 1, \dots, N_{gb} + N_{uav}\}$.

In the proposed network architecture, GUs communicate with the GBSs using Frequency Division Multiple Access (FDMA), which is an OMA scheme, whereas each UAV-based subnetwork adopts NOMA. In the NOMA-based UAV subnetworks, multiple associated GUs share the same frequency channel through power-domain multiplexing. Consequently, the UAV receives a superimposed signal consisting of the signals transmitted by the associated users. Successive Interference Cancellation (SIC) is employed at the UAV to decode the users' signals according to the adopted decoding order [18]. The use of different access schemes in the two subnetworks enables the proposed architecture to preserve the conventional access mechanism of the terrestrial network while exploiting the enhanced spectrum utilization provided by NOMA in the aerial subnetworks. Thus, the UAVs can be integrated into the existing MEC infrastructure without requiring fundamental modifications to the GBS-based communication structure.

The computation period is divided into N time slots, each having a duration of $\tau=T/N$, where the time slots are indexed by $n\in\{1,\dots,N\}$. To facilitate discrete-time resource allocation and trajectory optimization, the network conditions are assumed to remain unchanged within each time slot.

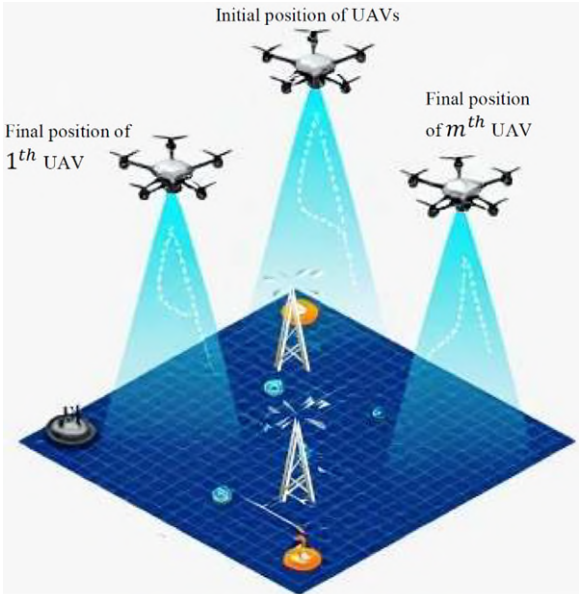


Fig. 1 Proposed two-tier hybrid aerial-terrestrial MEC network with multiple UAVs.

The channel power gain between i^{th} GU and m^{th} MEC server is modeled by considering the probabilistic Line-of-Sight (LoS) and Non-Line-of-Sight (NLoS) propagation conditions, together with the corresponding large-scale and small-scale fading effects [19]. The channel model accounts for the different propagation characteristics of GU–UAV and GU–GBS links. The specific channel parameters and propagation settings adopted in the simulations are presented in Section IV.

B. Task Offloading Scheme

We adopt a partial offloading strategy in which each GU can simultaneously perform a portion of its computational task locally and offload the remaining portion to MEC servers deployed on GBSs and UAVs. This approach provides additional flexibility in allocating computational workloads between local and edge computing resources [16].

Suppose $p_{i,s}[n]$ as the transmit power used by i^{th} GU in communicating with s^{th} MEC server in n^{th} time slot, and p_i^{max} is the upper limit of transmitting power for i^{th} GU, where:

$$\sum_s p_{i,s}[n] \leq p_i^{max} \qquad \forall i, \forall n. \tag{1}$$

For UAV-assisted offloading, NOMA is employed, and multiple GUs associated with the same UAV share the available spectrum. Therefore, the amount of data that can be offloaded from i^{th} GU to m^{th} UAV in the n^{th} time slot is determined by the achievable NOMA transmission rate, which accounts for the intra-group interference generated by the signals of the other simultaneously transmitting users.

Accordingly, the maximum number of bits that can be offloaded to m^{th} UAV by i^{th} GU during n^{th} time slot is given by

$$O_{i,m}[n] = \text{Ɓ}\tau \log_2\left(1 + \frac{p_{i,m}[n] g_{i,m}[n]}{I_{im}[n] + \sigma^2}\right), \tag{2}$$

where the intra-group interference is determined according to the adopted NOMA decoding order as $I_{im}[n] = \sum_{j \setminus i \,\&\, g_{j,m} < g_{i,m}}^{U} p_{j,m}[n] g_{j,m}[n]$. In addition, $\sigma^2 = \text{Ɓ}N_0$ denotes the variance of the additive white Gaussian noise (AWGN) at the receiver, N_0 represents the noise power spectral density, $g_{i,m}$ denotes the channel power gain between i^{th} GU and m^{th} UAV and Ɓ is the bandwidth allocated to the corresponding MEC server.

For GBS-assisted offloading, FDMA is employed as the OMA scheme. In contrast to NOMA, the available bandwidth is orthogonally divided among the GUs associated with each GBS, and no intra-group interference is considered. Thus, each GU is assigned a fraction of the available bandwidth according to the corresponding resource allocation constraint. The amount of data offloaded from i^{th} GU to b^{th} GBS during n^{th} time slot can consequently be expressed as:

$$O_{i,b}[n] = \frac{\mathcal{B}\tau}{N_{gu}} \log_2 \left(1 + \frac{p_{i,b}[n] g_{i,b}[n]}{\frac{\mathcal{B} N_0}{N_{gu}}} \right), \tag{3a}$$

and

$$p_{i,b}[n] = \frac{\mathcal{B} N_0}{N_{gu} g_{i,b}[n]} \left[\exp\left(N_{gu} \beta O_{i,b}[n] \right) - 1 \right], \tag{3b}$$

where $\beta \stackrel{\text{def}}{=} \ln(2)/(\mathcal{B}\tau)$.

Let $f_{i,s}[n]$ denote the computational capacity allocated by s^{th} MEC server to i^{th} GU, and let allocated to i^{th} GU, and the $f_i[n]$ denote the CPU frequency allocated to i^{th} GU for local computation during n^{th} time slot. The computational capacity constraints for i^{th} GU and s^{th} MEC server are given by:

$$f_i[n] \leq f_i^{max}, \qquad \forall i, \forall n \tag{4a}$$

and

$$\sum_i f_{i,s}[n] \leq f_s^{max}, \quad \forall s, \forall n \tag{4b}$$

where f_s^{max} and f_i^{max} represent the maximum computational capacity of s^{th} MEC server and the maximum CPU frequency of i^{th} GU, respectively. All computing devices are assumed to be equipped with a single-core CPU.

Let C_s and C_i denote the number of CPU cycles required to process one bit of input data at s^{th} MEC server and i^{th} GU respectively. The total number of bits processed for i^{th} GU during n^{th} time slot consists of the bits processed locally by the GU and the bits processed by the associated MEC servers. Accordingly, the number of processed bits can be expressed as:

$$d_i[n] = f_i[n] \frac{\tau}{C_i}, \tag{5a}$$

and

$$d_{i,s}[n] = f_{i,s}[n] \frac{\tau}{C_s}. \tag{5b}$$

A causality constraint is imposed to ensure that a MEC server can process only the data that have already been successfully offloaded by the corresponding GU. In other words, the number of bits processed by an MEC server for i^{th} GU up to a given time slot cannot exceed the cumulative amount of data offloaded to that server in the preceding time slots. Therefore, if D_i denotes the total amount of data associated with i^{th} GU, the cumulative processed data must satisfy the corresponding task-causality constraint.

$$D_i \leq \sum_n \sum_s (d_{i,s}[n] + d_i[n]). \qquad \forall i \tag{6}$$

Since the system operates in discrete time slots, the data offloaded during a given time slot become available for edge computation from the subsequent time slot. Consequently, no previously offloaded data are available for MEC processing during the first time slot. This causality relationship is incorporated into the task execution constraints.

Furthermore, once the computation period T expires, the remaining offloaded tasks are no longer considered for execution. Therefore, offloading data to MEC servers during the final time slot does not contribute to the completion of the corresponding computational tasks within the considered computation period [16]. Based on these assumptions, the task execution constraints for the GBS-based and UAV-based MEC servers are formulated as:

$$\sum_{j=1}^{n} d_{i,s}[j] \leq \sum_{j=1}^{n-1} O_{i,s}[j]. \quad \forall i, \forall n, \forall s \tag{7}$$

C. Energy Consumption Model

The total energy consumption of the proposed MEC system consists of three main components: computation energy, task offloading energy, and UAV propulsion energy [2]. For GUs, energy consumption is mainly associated with local computation and wireless task offloading. In contrast, UAVs consume energy for both computational processing and flight operations. For GBSs, the energy consumption considered in this work is associated with the execution of offloaded computational tasks [9].

At time slot n, the computation energy consumption for i^{th} GU and s^{th} MEC server is represented as follows [20]:

$$E_i[n] = k_i f_i[n]^3 \tau, \tag{8a}$$

$$E_s[n] = k_s \sum_i f_{i,s}[n]^3 \tau, \tag{8b}$$

where k_i and k_s are constants referred to as the effective switched capacitance of the CPU for i^{th} GU [4], [16], and s^{th} MEC server, respectively. Accordingly, the total computation energy consumption of the GUs and MEC servers over the entire computation period can be expressed as:

$$E_{comp}^{USER} = \sum_n \sum_i k_i f_i[n]^3 \, \tau, \tag{9a}$$

$$E_{comp}^{UAV} = \sum_n \sum_m k_m f_{i,m}[n]^3 \, \tau, \tag{9b}$$

$$E_{comp}^{BS} = \sum_n \sum_m k_b f_{i,b}[n]^3 \, \tau. \tag{9c}$$

Since GUs may offload their computational tasks to both UAV-based and GBS-based MEC servers, the total uplink energy consumed for task offloading is given by:

$$E_{comm}^{UAV} = \sum_n \sum_m \sum_i p_{i,m}[n] \tau, \tag{10a}$$

$$E_{comm}^{BS} = \sum_n \sum_b \sum_i p_{i,b}[n] \tau, \tag{10b}$$

$$E_{comm}^{USER} = E_{comm}^{UAV} + E_{comm}^{GBS}, \quad (10c)$$

where the corresponding transmit power represents the power required by i^{th} GU to offload data to s^{th} MEC server during n^{th} time slot.

In this work, the energy consumption associated with downlink transmission of computation results is neglected. This assumption is justified by the relatively small size of the computation results compared with the input data and by the fact that downlink communication energy is typically much smaller than the energy consumed for UAV propulsion and computation [13]. Therefore, the total energy consumption considered in the optimization problem consists of GU computation and uplink offloading energy, MEC-server computation energy, and UAV propulsion energy.

D. UAV Movement Model

The mobility of multiple UAVs is explicitly incorporated into the proposed optimization framework. At each time slot *n*, the position and velocity of m^{th} UAV are denoted by $\boldsymbol{r}_m[n]$ and $\boldsymbol{v}_m[n]$, respectively. Each UAV *m* starts from a predefined initial position and moves toward a predefined final position with a constant flight speed. Accordingly, the initial and final positions of m^{th} UAV are denoted by $\mathrm{r}_{\mathrm{m}}^{\mathrm{Init}}$, $\mathrm{r}_{\mathrm{m}}^{\mathrm{Final}}$, respectively, while its constant flight speed is denoted by v_{m}. The corresponding mobility constraints are given by:

$$\boldsymbol{r}_m[0] = \boldsymbol{r}_m^{Initial}, \ \boldsymbol{r}_m[N] = \boldsymbol{r}_{m,}^{Final} \quad \forall m \quad (11a)$$

$$\boldsymbol{v}_m[0] = \boldsymbol{v}_m^{Initial}, \ \boldsymbol{v}_m[N] = \boldsymbol{v}_{m,}^{Final} \quad \forall m \quad (11b)$$

$$\|\boldsymbol{r}_m[n] - \boldsymbol{r}_m[n-1]\| \leq \boldsymbol{v}_m[n]\tau \quad \forall m, n. \quad (11c)$$

To model UAV flight energy, we adopt the commonly used approach in [21], where UAV movement between two consecutive positions is modeled as uniform rectilinear motion with constant velocity and without acceleration. Under this assumption, the UAV trajectory is determined by its position at each time slot, while the flight speed remains constant throughout the computation period.

Accordingly, the propulsion energy consumed by m^{th} UAV during the flight is calculated as

$$E_{move}^{UAV} = \sum_n \sum_m E_{move}^m[n] = \tau \sum_n \sum_m \left(\frac{1}{2} W_m \|\boldsymbol{v}_m[n]\|^2\right) = \frac{1}{2} \tau W_m \sum_n \sum_m \left(\left\|\frac{\boldsymbol{r}_m[n]-\boldsymbol{r}_m[n-1]}{\tau}\right\|^2\right), \quad (12)$$

where the mass of m^{th} UAV is W_m. Under the constant-speed uniform-motion assumption, the propulsion energy in (12) is a convex quadratic function of the UAV displacement. This is in contrast to acceleration-based fixed-wing propulsion models, where the energy depends on velocity and acceleration and is generally non-convex. Consequently, no SCA is required on the propulsion term in the trajectory subproblem, which reduces the number of convex approximation stages compared with fixed-wing formulations.

III. PROBLEM FORMULATION

The primary objective of the proposed framework is to minimize the weighted energy consumption of the MEC network while satisfying the computational, communication, task offloading, and UAV mobility requirements. As discussed in Section II, the energy consumption associated with downlink transmission is assumed to be negligible and is therefore excluded from the optimization objective.

Accordingly, the joint optimization problem is formulated as follows:

$$\boldsymbol{p_0} \quad : \min_{\boldsymbol{f},\ \boldsymbol{p},\ \boldsymbol{r}} \ w_{user}\left(E_{comm}^{USER} + E_{comp}^{USER}\right) + w_{gbs}\left(E_{comp}^{GBS}\right) + w_{uav}\left(E_{comp}^{UAV} + \gamma E_{move}^{UAV}\right) \tag{13}$$

where $\boldsymbol{f}=\{f_i, f_{i,s}\}$, $\boldsymbol{p}=\{p_{i,s}\}$, $\boldsymbol{r}=\{\boldsymbol{r}_m\}$

Subject to:

C1: $f_i[n] \leq f_i^{max}, \qquad \forall\, i,n$

C2: $\sum_i f_{i,s}[n] \leq f_s^{max}, \qquad \forall\, s,m$

C3: $\sum_m \sum_b (p_{i,m}[n] + p_{i,b}[n]) \leq p_i^{max}, \quad \forall\, i,n$

C4: $\sum_{j=1}^{n} d_{i,s}[j] \leq \sum_{j=1}^{n-1} O_{i,s}[j], \quad \forall\, i,n,m$

C5: $D_i \leq \sum_n \sum_s (d_{i,s}[n] + d_i[n]), \quad \forall\, i$

*C*6: $\boldsymbol{r}_m[0] = \boldsymbol{r}_m^{Initial}, \quad \boldsymbol{r}_m[N] = \boldsymbol{r}_m^{Final}, \quad \forall\, m,n$

*C*7: $\|\boldsymbol{r}_m[n] - \boldsymbol{r}_m[n-1]\| \leq \boldsymbol{v}_m[n]\tau, \qquad \forall n, \forall m$

where $\boldsymbol{f}$, $\boldsymbol{p}$, and $\boldsymbol{r}$ denote the computational resource allocation, transmit power allocation, and UAV trajectory variables, respectively. The indices *i*, *s*, *m*, and *n* belong to the corresponding sets defined in the system model.

Constraints *C*1 and *C*2 regulate the computational resources allocated to GUs and MEC servers, respectively. Constraint *C*3 limits the total transmission power of each GU. Constraint *C*4 imposes the causality of task execution by ensuring that the amount of data processed by an MEC server does not exceed the amount of data previously offloaded to that server. Constraint *C*5 guarantees that the computational task of each GU is completed within the prescribed computation period. Finally, constraints *C*6 and *C*7 specify the UAV mobility requirements, including the predetermined initial and final positions and the maximum displacement during each time slot.

The nonnegative weighting coefficients w_{user}, w_{gbs}, and w_{uav} determine the relative importance assigned to the energy consumption of GUs, GBSs, and UAVs, respectively. Since the propulsion energy consumption of UAVs is generally much larger than their computation and communication energy consumption, the weighting coefficient $\boldsymbol{\gamma}$ is introduced to appropriately balance the contribution of UAV propulsion energy in the objective function.

The resulting optimization problem jointly determines the computational resource allocation, transmit power allocation, and trajectories of multiple UAVs. The strong coupling among these variables, together with the nonlinear rate expressions and UAV mobility constraints, makes the formulated problem non-convex. Therefore, conventional convex optimization methods cannot be directly applied to solve the original problem. In the following section, appropriate transformation and convexification techniques are employed to decompose the original problem into tractable subproblems, which are solved iteratively to obtain an efficient solution.

IV. SOLUTION ALGORITHM FOR THE OPTIMIZATION PROBLEM

Determining the global optimum of the formulated non-convex problem is generally computationally intractable. Therefore, an iterative optimization framework is developed to obtain a locally optimal solution. The original problem is decomposed into two coupled sub-problems:

- **Resource Management Sub-problem:** Joint optimization of radio and computational resource allocation for given UAV trajectories.
- **UAV Trajectory Optimization Sub-problem:** Optimization of the trajectories of multiple UAVs for given radio and computational resource allocation. Because the propulsion energy is convex in the UAV displacement, the trajectory subproblem does not require SCA on the propulsion term, which reduces the number of convex approximation stages and the per-iteration computational cost compared with acceleration-based fixed-wing formulations.

The two sub-problems are solved alternately until the change in the objective function between two consecutive iterations falls below a predefined convergence threshold. The overall optimization procedure is summarized in Algorithm 1.

A. Joint Optimization of Radio and Computational Resource

For given UAV trajectories, the original problem can be reduced to the joint optimization of communication and computational resources. The corresponding sub-problem is formulated as:

$$\boldsymbol{p_1}: \quad \min_{\boldsymbol{f},\boldsymbol{p}} w_{user}\left(E_{com\,m}^{USER} + E_{comp}^{USER}\right) + w_{gbs}\left(E_{comp}^{GBS}\right) + w_{uav}\left(E_{comp}^{UAV}\right) \tag{14}$$

where $\boldsymbol{f} = \{f_{user}, f_{gbs}, f_{uav}\}$, $\boldsymbol{p} = \{p_{i,m}, p_{i,b}\}$,

Subject to:

C1~ C5.

The objective function of problem $\boldsymbol{p_1}$ consists of several energy consumption components. According to (9), the computation energy terms associated with GUs, UAVs, and GBSs are polynomial functions of CPU frequencies with positive coefficients and are therefore convex. Furthermore, the total communication energy is composed of the offloading energy associated with GBSs and UAVs.

Based on Eqs. (3*b*) and (10*b*), the energy consumption corresponding to GU–GBS communications is expressed as a sum of exponential functions with positive coefficients and is therefore convex.

For GU–UAV communications, by substituting the transmission power expression derived from Eq. (10*a*) into the uplink NOMA transmission model in (2), the offloading energy can also be expressed as a sum of exponential functions with positive coefficients. The detailed proof is provided in Appendix A.

Accordingly, the transmission energy associated with UAV communications in time slot *n* can be expressed as

$$\sum_i p_{i,m}[n] = \sigma^2 \sum_{i=0}^{N_{gu}} (-l_{i+1,m}[n] + l_{i,m}[n]) \; exp\big(\beta x_{i,m}[n]\big), \tag{15}$$

which is a convex function with respect to the optimization variables. Therefore, the overall objective function of problem $\boldsymbol{p_1}$ is convex.

The effect of variable transformations on the associated constraints is also analyzed in Appendix A. By introducing auxiliary variables, several constraints are reformulated into equivalent expressions. However, some constraints remain non-convex after the transformations. To address this issue, the Successive Convex Approximation (SCA) technique [8], [22] is employed, where first-order Taylor approximations are used to obtain convex surrogate functions.

Consequently, the original non-convex sub-problem is transformed into a convex optimization problem of the following form:

$$\boldsymbol{p_{1.1}}: \; \min_{\boldsymbol{f},\boldsymbol{x}} \; w_{user}\{\sigma^2 . \sum_m \sum_i \sum_n (-l_{i+1,m}[n] + l_{i,m}[n]) exp(\beta . x_{i,m}[n]) \tag{16}$$

$$+ \frac{\sigma^2}{N_{gu}} \sum_b \sum_i \sum_n l_{i,b}[n] \; (exp\big(U.\beta.O_{i,b}[n]\big) - 1) + E_{comp}^{USER}\} + w_{uav} E_{comp}^{UAV} + w_{gbs} E_{comp}^{GBS}$$

where $\boldsymbol{f} = \{f_{user}, f_{gbs}, f_{uav}\}$, and $\boldsymbol{x} = \{x_{i,m}, O_{i,b}\}$

Subject to: $C1$, $C2$, $C3''$, $C4'$, $C5$

Since both the objective function and all constraints of $\boldsymbol{p_{1.1}}$ are convex, the problem can be efficiently solved using standard convex optimization tools such as CVX [23].

The solution is obtained iteratively, where the expansion points used in the Taylor approximations are updated according to the solution obtained in the previous iteration until convergence is achieved.

B. Multi-UAV Trajectory Optimization

In this subsection, UAV trajectories are optimized under fixed communication and computational resource allocation. Since task offloading to GBSs is independent of UAV trajectories and the computational resources have already been determined, the corresponding energy components remain constant during this stage. Therefore, the trajectory optimization sub-problem can be formulated as:

$$\boldsymbol{p_2}: \quad \min_{\boldsymbol{r}} w_{user}(E_{comm}^{UAV}) + w_{uav}(\gamma E_{move}^{UAV}), \tag{17}$$

where $\boldsymbol{r} = \{\boldsymbol{r}_m\}$,

*Subject to C*6, *C*7.

The trajectories of UAVs directly affect both the propulsion energy and the wireless channel quality between GUs and UAVs. Consequently, UAV movement influences the transmission energy required for task offloading.

Based on the path loss model, the communication energy component associated with GU–UAV transmissions can be rewritten as:

$$E_{comm}^{UAV} = \sum_m \sum_i \sum_n \mu(m,i,n)\bar{L}_{i,m}[n], \tag{18}$$

where the corresponding coefficients, $\mu(m,i,n)$, are treated as constants.

Due to the nonlinear relationship between the UAV positions and the corresponding channel conditions, the trajectory optimization sub-problem $\boldsymbol{p_{2.1}}$ remains non-convex. To obtain a tractable formulation, the path-loss-related term is approximated using a quadratic function. Specifically, the corresponding path-loss term is expressed as:

$$\bar{L}_{i,m}[n] \approx \tilde{L}_{i,m}^{approx}[n] = q_1\, d_{i,m}[n]^2 + q_2 d_{i,m}[n] + q_3\,, \tag{19}$$

where q_1, q_2 and q_3 are fitting coefficients determined to provide a satisfactory approximation of the original path-loss function. The coefficients are selected such that $q_1, q_2 \geq 0$, thereby ensuring that the resulting quadratic approximation is convex. This approximation transforms the corresponding non-convex component into a tractable convex form while maintaining an acceptable approximation accuracy. This approximation provides an accurate representation of the path loss model while preserving computational tractability [16].

As a result, the objective function becomes convex with respect to the UAV trajectory variables. The reference trajectory is iteratively updated until convergence.

Accordingly, the trajectory optimization problem $\boldsymbol{p_{2.1}}$ is reformulated as:

$$\boldsymbol{p_{2.1}}: \min_{\boldsymbol{r}} \quad w_{user} \sum_m \sum_i \sum_n \mu(m,i,n)\bar{L}_{i,m}[n] + w_{uav}(\gamma E_{move}^{UAV}), \tag{20}$$

where $\boldsymbol{r} = \{\boldsymbol{r}_m\}$,

Subject to: C6, and C7, $\forall n, \forall m$

Since both the objective function and constraints of $\boldsymbol{p_{2.1}}$ are convex, it can be efficiently solved using CVX.

C. Joint Optimization of Radio and Computation Resources and UAV Trajectories

The joint optimization of the two sub-problems, namely computation and radio resources, and UAV trajectories optimization, can be achieved by iteratively solving them, as outlined in Algorithm 1.

Algorithm 1 Joint Optimization of Radio and Computation Resources and UAV Trajectories

Initialization:
Initialize the GU locations, GBS locations, UAV initial and final positions, UAV trajectories, system parameters, and computation tasks

1. Given the GU locations, GBS locations, and initial UAV trajectories, calculate the channel gains between each GU and the corresponding GBS/UAV in each time slot.
2. For each UAV-MEC server and time slot, determine the NOMA decoding order according to the channel gains of the associated GUs.
3.Given the initial UAV trajectories, solve the convexified resource-management sub-problem $\boldsymbol{p_{1.1}}$ using CVX and obtain the initial radio and computational resource allocation.
4.Set the iteration index λ=0 and evaluate the corresponding weighted system energy.
5. **repeat**
6.Given the current radio and computational resource allocation, solve the trajectory optimization sub-problem $\boldsymbol{p_{2.1}}$ using the quadratic approximation and CVX, and obtain the updated UAV trajectories.
7. Update the channel gains according to the new UAV trajectories.
8. Given the updated UAV trajectories, solve the convexified resource-management sub-problem $\boldsymbol{p_{1.1}}$ using CVX and obtain the updated radio and computational resource allocation.
9. Evaluate the weighted system energy using the updated resource allocation and UAV trajectories.
10. set $= \lambda + 1$.
11. the change in the weighted system energy between two consecutive iterations satisfies

$$|\mathbf{utilitySeq_p_0}(\boldsymbol{\lambda}) - \mathbf{utilitySeq_p_0}(\boldsymbol{\lambda - 1})| \leq \boldsymbol{\epsilon}.$$

12. Calculate the corresponding transmission powers and other system variables based on the final resource allocation and channel gains.
13. return $\boldsymbol{p_{i,m}}, \boldsymbol{p_{i,gbs}}, \boldsymbol{f_{user}}, \boldsymbol{f_{gbs}}, \boldsymbol{f_{uav}}, \boldsymbol{r_{uav}}$.

V. PERFORMANCE EVALUATION AND SIMULATION RESULTS

A. Simulation Setup

The performance of the proposed optimization framework is evaluated through simulations. All simulations are implemented in MATLAB R2023a on a computer equipped with an Intel Core i5-1035G7 processor operating at 1.20 GHz and 8 GB of RAM.

We consider a network with 10 GUs, each having a computational task of 300 Mbits to be completed within a time horizon of 100 s. The GUs are uniformly distributed over a 1×1 km^2 area. The network consists of five MEC servers, including three UAV-based MEC servers and two GBS-based MEC servers. The UAVs operate at an altitude of 50 m. Their initial positions are given by $\boldsymbol{r}_m^{UAV}[0] =$ (10,10,50), while their predetermined final positions are:

- $\boldsymbol{r}_1^{UAV}[N] =$ UAV 1: (10,1000,50),
- $\boldsymbol{r}_2^{UAV}[N] =$ UAV 2: (1000,10,50),
- $\boldsymbol{r}_3^{UAV}[N] =$ UAV 3: (1000,1000,50).

The GBSs are located at:

- $\boldsymbol{r}_1^{GBS} =$ (1000/3,1000/3,19),
- $\boldsymbol{r}_2^{GBS} =$ (2000/3, 2000/3,19).

TABLE III- SIMULATION PARAMETERS

Parameters	Values [1] ,[2],[16],[24]
Time horizon	T = 100 s
Altitudes of UAV	H = 50 m
speed of UAVs	v_{max} = 20 m/s
Time slot size	$\boldsymbol{\tau}$= 5 s
Maximum transmit power of each GU	p_{max}= 20 w
System bandwidth (B)	4 MHz
Carrier frequency (fc)	
GU–UAV:	5.8GHz
GU–GBS:	3.5GHz
PSD of noise (N0)	10^{-17}W/Hz
Process density (C)	10^3 cycles/bit
Effective switched capacitance (k)	10^{-28}
Maximum CPU frequency of GUs (f_{max}^{USER})	1 GHz
Maximum CPU frequency of MEC servers (f_{max}^{UAV}) and (f_{max}^{GBS})	10 GHz
threshold (ϵ)	1
Mass of UAVs (W)	10 kg
UAVs' weight factors γ	1×10^{-4}

The total computation horizon is divided into 20 time slots, each with a duration of 5 s. The maximum UAV speed is set to 20 m/s. The weighting coefficients associated with GUs, GBSs, and UAVs are set to w_{user} = 0.6, w_{gbs}= 0.3, and w_{uav} = 0.1, respectively. The remaining simulation parameters are listed in Table III. Here, ϵ denotes the convergence threshold used as the stopping criterion for the iterative optimization algorithm. The iterative process is terminated when the absolute difference between the weighted utility values obtained in two consecutive iterations falls below ϵ, indicating convergence of the algorithm.

Two channel models are considered for the GU–UAV and GU–GBS links. For the GU–UAV links, a probabilistic LoS/NLoS channel model based on the ITU-R framework for an urban environment is adopted [19]. The model accounts for path loss and small-scale fading, with Rician and Rayleigh fading considered for LoS and NLoS conditions, respectively. The carrier frequency of the UAV links is set to 5.8 GHz and urban path loss exponents (2.1 for LoS, 3.0 for NLoS). For the GU–GBS links, a terrestrial urban NLoS channel model is considered at a carrier frequency of 3.5 GHz, with a path-loss exponent of 3.7 and Rayleigh fading. Figure 2 illustrates the total path loss between all GUs and each MEC server over the considered time slots. The network consists of three UAV-based MEC servers and two GBS-based MEC servers; accordingly, five curves are presented in the figure. The path loss associated with each UAV varies over time as the UAV moves along its trajectory, resulting in time-varying channel conditions. In contrast, the path loss associated with the GBSs remains relatively stable because the GBSs are stationary. As observed, the UAV-based links generally experience lower total path loss than the GBS-based links. This difference can be mainly attributed to the higher probability of LoS propagation offered by the elevated UAVs. The more favorable channel conditions provided by the UAVs can reduce the transmission power required for task offloading and, consequently, contribute to lower energy consumption at the GUs.

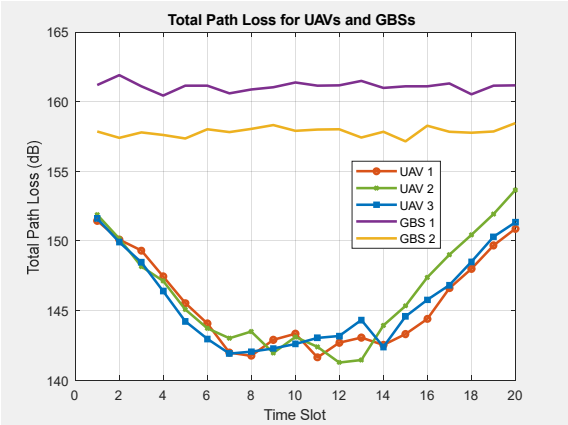


Fig. 2. Total path loss between the GUs and the UAV/GBS MEC servers.

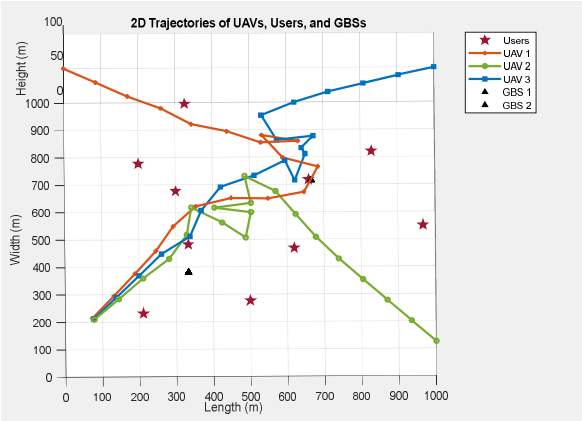


Fig. 3. Optimized UAV trajectories and spatial distribution of GUs and GBSs: 2D view

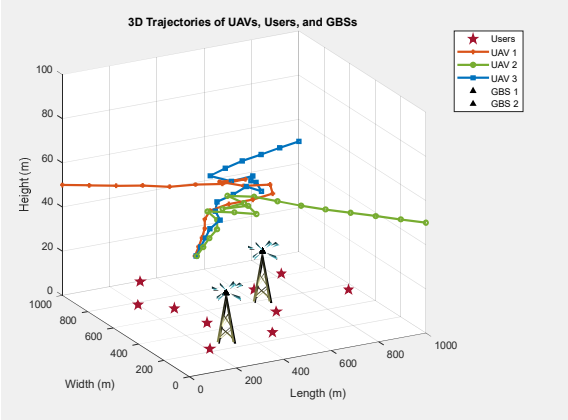
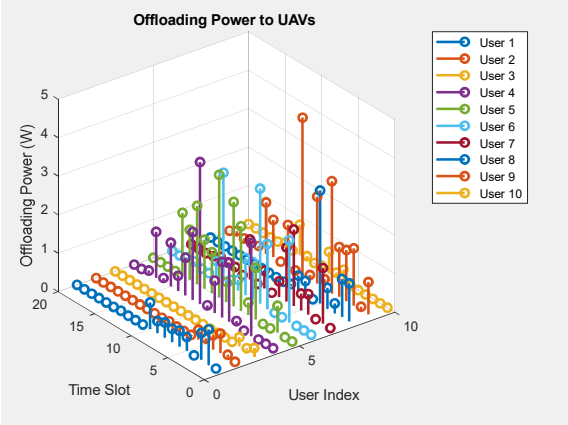


Fig. 4. Optimized UAV trajectories and spatial distribution of GUs and GBSs: 3D view

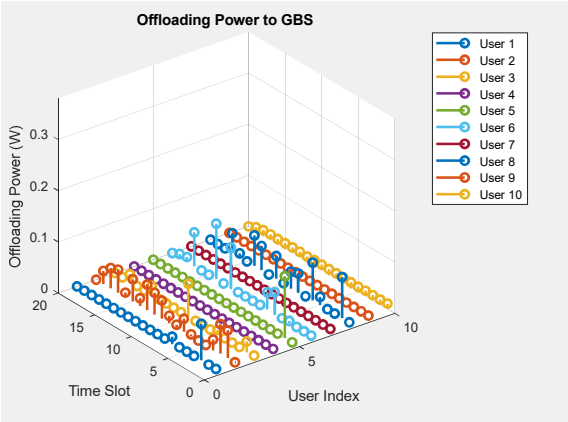
Figures 3 and 4 illustrates the optimized trajectories of the three UAVs together with the spatial distribution of the GUs and the locations of the two GBSs. Both the three-dimensional and two-dimensional views are presented to provide a clearer representation of the UAV mobility within the considered service area. As shown, the UAVs move from their predefined initial positions toward their corresponding final positions while adapting their trajectories according to the spatial distribution of the

GUs. The resulting trajectories allow the UAVs to approach different groups of GUs during the flight, thereby providing more favorable GU–UAV communication conditions while satisfying the imposed mobility constraints. In contrast, the GBSs remain fixed throughout the considered time horizon.

Figs. 5 and 6 illustrate the GU offloading power allocation toward the UAV-based and GBS-based MEC servers. The results show that the offloading power varies across users and time slots, particularly for the UAV-based links, due to the mobility-induced changes in GU–UAV channel conditions. The higher probability of LoS propagation and the mobility of UAVs provide more favorable aerial communication conditions, allowing the optimization framework to dynamically allocate a larger portion of the offloading activity to the UAV subnetworks during appropriate time slots. Meanwhile, the GBSs provide relatively stable and complementary terrestrial resources. Overall, the results demonstrate the ability of the proposed framework to dynamically exploit the complementary aerial and terrestrial MEC resources.



a. GU-to-UAV offloading



b. GU-to-GBS offloading

Fig. 5. Offloading transmission power allocated to individual GUs over the considered time horizon: (a) GU-to-UAV offloading; (b) GU-to-GBS offloading.

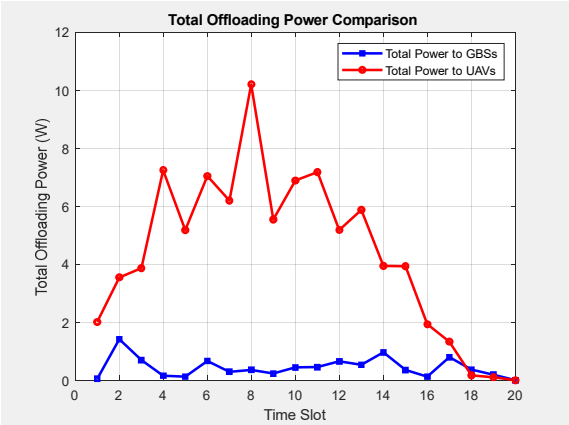


Fig. 6. Total GU offloading transmit power toward UAV-based and GBS-based MEC servers over the considered time horizon.

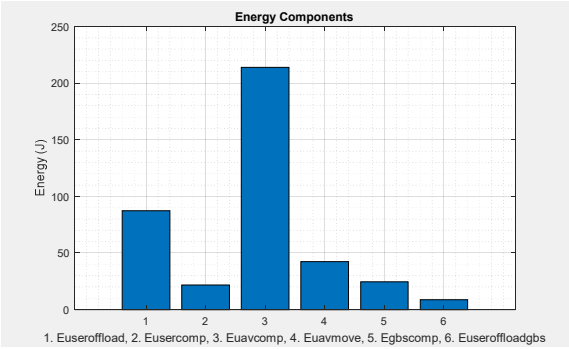


Fig. 7. Composition of system energy consumption across user computation, task offloading, UAV computation, UAV propulsion, and GBS computation in the proposed UAV-assisted MEC network.

The composition of energy consumption for task computing, task offloading and UAV flight as three main components of UAV-aided MEC network energy consumer depict in Fig. 7. The results highlight the role of UAVs in reducing the energy consumption of GUs. Due to the favorable propagation conditions and improved channel gains provided by the UAVs, offloading tasks through UAV-based links can require less transmission energy at the user side than transmitting the same amount of data through terrestrial links with higher path loss. Consequently, the optimization framework tends to exploit UAV-based edge resources for task offloading, despite the additional energy required for UAV computation and propulsion. This behavior is particularly relevant because the energy consumption of GUs is assigned a higher priority in the weighted objective function (w_{user}=0.6), compared with the energy consumption of UAVs (w_{uav}=0.3) and GBSs (w_{gbs}=0.1). Thus, the proposed optimization establishes a system-level trade-off in which additional energy expenditure at the UAVs can be justified by a reduction in user-side energy consumption.

Fig. 8 depicts the convergence behavior of the weighted system energy during the iterative optimization process. Starting from approximately 180.3, the objective value gradually decreases to about 150.24 after four iterations, representing an overall reduction of approximately 16.6%. This progressive decrease reflects the effectiveness of alternately optimizing resource allocation and UAV

trajectories, allowing the algorithm to progressively improve the system-wide energy efficiency. The objective function exhibits a nearly monotonic decreasing trend and reaches a stable value within a small number of iterations. This behavior demonstrates the convergence and numerical stability of the proposed iterative optimization framework. Moreover, achieving convergence within four iterations suggests that the proposed method can provide an effective trade-off between solution quality and computational effort.

Fig. 9 illustrates the distribution of the total energy consumption among the different components of the proposed UAV-assisted MEC network. As shown, the largest share corresponds to the energy consumed by GUs for offloading tasks to UAVs, followed by the computation energy of UAVs. This indicates that UAV-based task offloading constitutes a significant part of the overall energy budget of the system. The energy consumed by local computation at GUs represents a relatively small portion of the total energy consumption. This behavior is consistent with the objective of the proposed weighted optimization framework, in which reducing the energy consumption of GUs is assigned a relatively high priority. The optimization therefore tends to exploit UAV-based edge resources when their favorable communication conditions can reduce the energy expenditure of GUs.

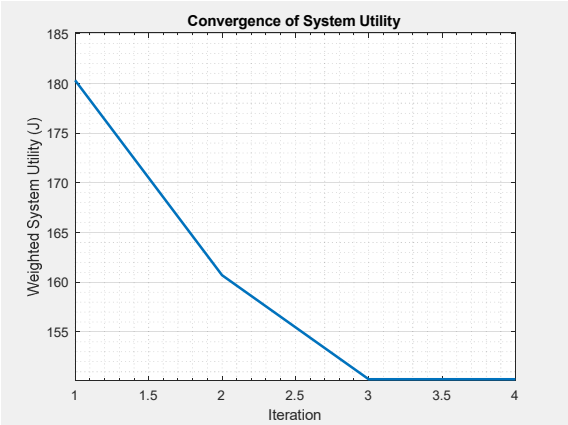


Fig. 8. The convergence behavior of the system's weighted utility.

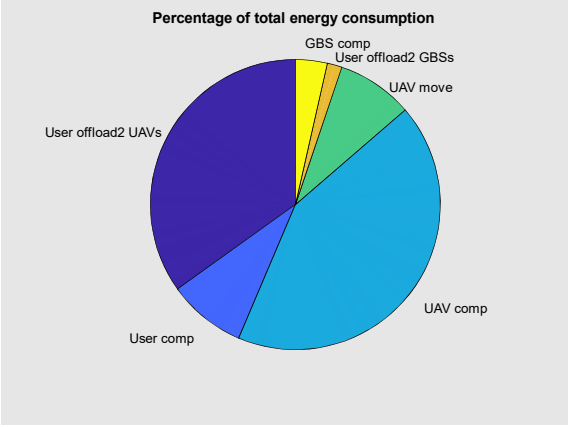


Fig. 9. Distribution of total energy consumption among different components of the proposed UAV-assisted MEC network.

At the same time, UAV computation and propulsion account for noticeable portions of the total energy consumption, reflecting the energy cost associated with utilizing aerial edge resources. In contrast, the energy consumed for offloading to GBSs and computation at GBSs is relatively small. Overall, the results demonstrate a system-level energy trade-off: the proposed framework utilizes the aerial resources despite their associated computation and mobility costs in order to reduce the energy consumption of user devices and improve the overall weighted energy efficiency of the network resources.

B. Comparison with UAV less Network without

To evaluate the impact of UAV deployment on the energy consumption of the proposed network, an additional simulation scenario is considered in which the UAVs are removed from the proposed architecture. In this scenario, the remaining network configuration is kept consistent with the proposed system, while the GBSs serve as the only external MEC servers. The FDMA-based access mechanism for GU–GBS communications is retained, whereas the UAV-based NOMA links are removed. The resulting energy consumption is then compared with that of the proposed UAV-assisted network.

Fig. 10 illustrates the energy consumption of the network when UAVs are not deployed and the GBSs are the only external MEC servers. Compared with the proposed UAV-assisted configuration shown in Fig. 7, the energy consumed by GUs for local computation and task offloading to GBSs is considerably higher. This difference highlights the contribution of UAVs as additional and geographically closer MEC resources. The shorter and more favorable GU–UAV links can reduce the transmission energy required for task offloading, while the availability of UAV-based computing resources also reduces the computational burden on GUs.

It should be noted that, in the no-UAV scenario, the maximum amount of data that can be processed for each GU is approximately 120 Mbits, compared with 300 Mbits in the proposed UAV-assisted configuration. This difference results from the computational-resource limitations of the GBS-only configuration and is taken into account in the corresponding simulation. Therefore, the comparison is intended to evaluate the impact of adding UAV-based MEC resources to the proposed network under the considered system constraints. The results indicate that removing UAVs substantially increases the energy consumption associated with GU computation and task offloading. Although introducing UAVs incurs additional energy consumption for UAV computation and propulsion, these costs are accompanied by a reduction in the energy expenditure of GUs. This trade-off demonstrates the effectiveness of integrating UAVs into the proposed MEC architecture for improving the overall energy efficiency of the considered network.

The comparison of Figs. 9 and 11 highlights the significant impact of UAV deployment on the energy consumption profile of the network. In the proposed UAV-assisted MEC network, the energy consumed by GUs for local computation and task offloading is substantially reduced compared with the network without UAVs. This improvement can be attributed to the shorter and more favorable GU–

UAV communication links, which reduce the transmission energy required for task offloading. As a result, a larger portion of the computational workload can be efficiently transferred to UAV-based MEC servers, relieving GUs from local computation and reducing their overall energy consumption. Although UAV deployment introduces additional energy costs associated with UAV computation and propulsion, these costs are effectively balanced against the reduction in GU energy consumption through the joint optimization framework. Therefore, the comparison demonstrates the effectiveness of incorporating UAVs as aerial MEC servers for improving the energy efficiency of the considered network.

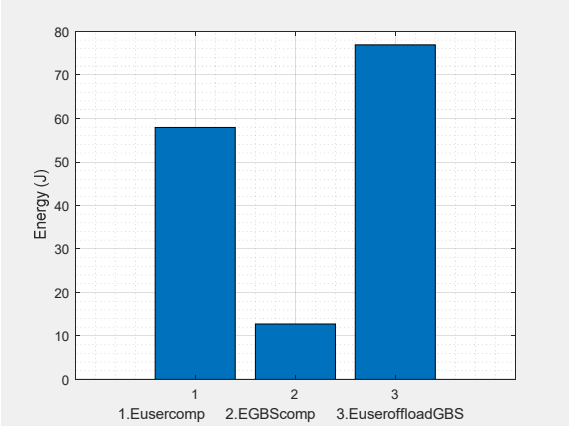


Fig. 10. Composition of system energy consumption for task computation and offloading in the proposed MEC network without UAVs

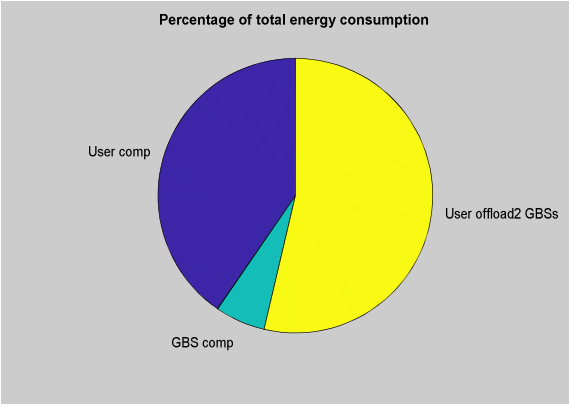


Fig. 11. Distribution of total energy consumption among the network components in the proposed MEC network without UAVs.

VI. CONCLUSIONS

The optimization problem formulated in this paper is highly non-convex due to the strong coupling among communication, computation, offloading, and UAV mobility variables. To address this challenge, the problem was decomposed into resource management and UAV trajectory scheduling

subproblems, which were solved iteratively using convexification and successive convex approximation techniques. The resulting approach provides a tractable solution while accounting for the energy costs associated with user computation and transmission, MEC computation, and UAV propulsion. The constant-speed rotary-wing propulsion model and the tier-specific channel modeling adopted in this work structurally simplify the trajectory subproblem and reduce the number of convex approximation stages required by the iterative algorithm.

Simulation results demonstrated the effectiveness of the proposed framework. The weighted system energy decreased from approximately 180.3 to 150.24 within four iterations, corresponding to a reduction of about 16.6%, indicating stable convergence of the iterative optimization process. The energy-consumption analysis further showed that UAV-based edge resources can provide favorable communication conditions and consequently reduce the energy required by GUs for task offloading. Although UAV computation and propulsion introduce additional energy costs, their integration enables a favorable system-level trade-off, particularly when reducing GU energy consumption is given higher priority in the optimization objective.

The comparison with a reference network without UAVs further highlights the potential of aerial edge resources to improve the energy efficiency of the user side by providing additional and more favorable communication and computing resources. Overall, the results demonstrate that combining existing terrestrial MEC infrastructure with strategically deployed UAV-based edge resources and hybrid OMA/NOMA access can provide an effective approach for energy-aware MEC network design

FUNDING
The authors received no financial support for the research, authorship, and/or publication of this article.

APPENDIX A.

A.1: *Convexity Analysis of the UAV Offloading Energy* E_{comm}^{USER}.

This appendix establishes the convexity of the uplink offloading energy associated with the UAV-based subnetwork. The analysis is based on the NOMA transmission model introduced in Section II. By introducing suitable auxiliary variables and exploiting the decoding order of the users, the UAV offloading energy can be represented in a form involving exponential functions with non-negative coefficients. This representation is then used to establish the convexity of the corresponding objective component.

Starting from Eq. (2), we introduce the following auxiliary quantities,

$$\beta \triangleq \ln(2)/(B\tau), \tag{21a}$$

and

$$M_{i,m}[n] \triangleq \sum_{l=1}^{i} p_{l,m}[n] g_{l,m}[n] + \sigma^2. \tag{21b}$$

Using these definitions, the offloaded data expression in Eq. (2) can be rewritten as:

$(\exp(O_{i,m}[n]\beta) - 1)\, M_{i-1,m}[n] = p_{i,m}[n] g_{i,m}[n]$. (22)

Furthermore, by substituting the definition of the auxiliary variable $M_{i,m}[n]$, and rearranging the resulting expression, we obtain:

$M_{i,m}[n] - M_{i-1,m}[n] = p_{i,m}[n] g_{i,m}[n]$, $\quad i \in \{2, 3, \ldots, U\}$. (23)

Combining (21) and (22), the amount of data offloaded by the users can therefore be expressed recursively as:

$M_{i,m}[n] = \exp(\beta O_{i,m}[n]) M_{i-1,m}[n]$, $\quad i \in \{2, 3, \ldots, U\}$. (24)

For the first user by index *i*=1, the corresponding initial conditions are given by:

$M_{1,m}[n] = p_{1,m}[n] g_{1,m}[n] + \sigma^2$, (25*a*)

and

$\sum_{j \setminus 1 \,\&\, g_{j,m} < g_{1,m}} p_{j,m}[n] g_{j,m}[n] = 0$, (25*b*)

consequently, we obtain:

$M_{1,m}[n] = \sigma^2 \exp(\beta\, O_{1,m}[n])$, (26)

which has the same recursive structure as (24). Expanding this relationship over the complete set of users gives:

$M_{i,m}^{UAV}[n] = \sigma^2 \exp(\beta \sum_{l=1}^{i} O_{l,m}^{UAV}[n])$, $\quad \forall i$. (27)

To simplify the subsequent derivation, we define the following auxiliary variable,

$x_{i,m}[n] \stackrel{\text{def}}{=} \sum_{l=1}^{i} O_{l,m}[n]$. (28)

Accordingly, the complete expression for $M_{i,m}[n]$ can be written as:

$M_{i,m}[n] = \sigma^2 \exp(\beta x_{i,m}[n])$, $\quad \forall i$ (29)

where the introduced cumulative quantity, $x_{i,m}[n]$, represents the cumulative amount of data offloaded to the m^{th} UAV by users with indices from 1 to *i* during n^{th}time slot.

Using Eqs. (23) and (29), the transmit power required by i^{th} user to offload data to m^{th} UAV during n^{th} time slot can be written as:

$\sum_i p_{i,m}[n] =$

$\sum_i \frac{\sigma^2}{g_{i,m}[n]} (\exp(\beta\, x_{i,m}[n]) - \exp(\beta\, x_{i-1,m}[n])) = \sigma^2 \sum_i \left(-\frac{1}{g_{i+1,m}[n]} + \frac{1}{g_{i,m}[n]} \right) \exp(\beta\, x_{i,m}[n])$. (30)

For the uplink NOMA transmission, the users are ordered according to their channel gains. In accordance with the decoding order adopted in the system model, the channel gains satisfy,

$g_{1,m}[n] \leq \ldots \leq g_{U,m}[n]$. Under this ordering, the coefficients associated with the exponential terms appearing in (30) are non-negative ($(\frac{-1}{g_{i+1,m}[n]} + \frac{1}{g_{i,m}[n]}) \geq 0$). Substituting the definition, $l_{i,m}[n] = \frac{1}{g_{i,m}[n]}$, and considering the corresponding special case, $l_{0,m}[n] = l_{U+1,m}[n] = 0$, Eq. (30) can consequently be expressed in the following form:

$$\sum_i p_{i,m}[n] = \sigma^2 \sum_{i=0}^{U} (-l_{i+1,m}[n] + l_{i,m}[n]) \exp(\beta x_{i,m}[n]). \quad (31)$$

The resulting expression is a nonnegative weighted sum of exponential functions with respect to the optimization variables. Since the exponential function is convex and a nonnegative weighted sum of convex functions remains convex, the UAV offloading-energy component is therefore convex with respect to the variables of the resource-management subproblem. Accordingly, together with the convex computation-energy terms and the GBS offloading-energy component discussed in Subsection III-A, the objective function of the resource-management subproblem is convex.

A.2: ***Reformulation of the Related Constraints***

The auxiliary variable introduced in Eq. (28) also provides a convenient representation for the variables appearing in the associated constraints. In particular, the original variables $p_{i,m}[n]$ and $O_{i,m}[n]$ can be expressed in terms of $x_{i,m}[n]$. From Eq. (28), the relationship between the cumulative and individual offloaded data is given by:

$$x_{i,m}[n] - x_{i-1,m}[n] = O_{i,m}[n]. \quad (32)$$

To explicitly represent the NOMA decoding order, we subsequently define a ranking function, $\Omega(i,n,m)$, that identifies the position of i^{th} user among the users associated with m^{th} UAV in the n^{th} time slot. Accordingly, the amount of data offloaded by i^{th} user to m^{th} UAV during n^{th} is expressed as:

$$O_{i,m}[n] = x_{\Omega(i,n,m),m}[n] - x_{\Omega(i,n,m)-1,m}[n]. \quad (33)$$

After this substitution, constraints $C3$ and $C4$ in $\boldsymbol{p_1}$ optimization problem can be reformulated in terms of the newly introduced variables $C3', C4'$, as follows:

$$C3': 0 \leq \sum_m \frac{\sigma^2}{g_{\Omega(i,n,m),m}[n]} \{\exp(\beta x_{\Omega(i,n,m),m}[n]) - \exp(\beta x_{\Omega(i,n,m)-1,m}[n])\} + \sum_b p_{i,b}[n] \leq p_i^{max}$$
$$\forall i, \forall n$$

$$C4': \sum_{j=1}^{n} f_{i,m}[j]\tau / C_m \leq \sum_{j=1}^{n-1} \left((x_{\Omega(i,n,m),m}[n]) - (x_{\Omega(i,n,m)-1,m}[n]) \right), \quad \forall i, \forall n, \forall m.$$

The resulting formulation in constraint $C3'$, however, contains terms involving the difference between exponential functions. Therefore, the convexity of these constraints cannot be directly established from their original form. To obtain a tractable convex approximation, the SCA method is

employed [2], [4]. Specifically, each relevant exponential term is approximated locally using its first-order Taylor expansion around the solution obtained in the previous iteration.

Consider the exponential function $y(x) = exp(\beta x)$, at a given feasible point x_0, its first-order Taylor approximation is given by:

$$\tilde{y}(x|x_0) = \mathrm{y}(x_0) + \frac{\partial y(x)}{\partial x}(x - x_0) = exp(\beta x_0) + \beta\, exp(\beta x_0)\,(x - x_0)\,. \quad (34)$$

The resulting approximation is an affine function of x. By replacing the appropriate exponential term in $C3'$ with its first-order Taylor approximation, the corresponding convex surrogate constraint $C3''$ is obtained as:

$$C3'': 0 \leq \sum_m \frac{1}{g_{\Omega(i,n,m),m}[n]} \{\mathrm{y}\big(x_{\Omega(i,n,m),m}[n]\big) - \tilde{y}\big(x_{\Omega(i,n,m)-1,m}[n] \mid \hat{x}^{\lambda-1}_{\Omega(i,n,m)-1,m}[n]\big)\} +$$

$$\sum_b \frac{1}{N_{gu} g_{i,b}[n]} [exp\big(U\beta O_{i,b}[n]\big) - 1] \leq \frac{p_i^{max}}{\sigma^2}, \qquad \forall i, \forall n$$

where, $\hat{x}^{\lambda-1}_{\Omega(i,n,m)-1,m}[n]$ represents the solution to $x_{\Omega(i,n,m)-1,m}[n]$ obtained at the $(\lambda-1)^{th}$ SCA iteration repetition and is used as the expansion point for constructing the next convex approximation.

The resulting approximation in $C3''$ preserves the tractable structure required by the convex optimization procedure. In particular, the exponential terms are replaced by their first-order affine approximations at the current iteration point, while the remaining GBS-related transmission terms retain their convex form. Consequently, the resulting constraints form a convex feasible set for each SCA iteration. Therefore, the resource-management subproblem can be solved iteratively by updating the expansion point using the solution of the previous iteration. This procedure produces a sequence of convex optimization problems that can be efficiently solved using CVX. The iterative process continues until the convergence criterion defined in the main algorithm is satisfied.

REFERENCES

[1] S. Huang, J. Zhang, and Y. Wu, "Altitude Optimization and Task Allocation of UAV-Assisted MEC Communication System," *Sensors*, vol. 22, p. 8061, 2022.

[2] Y. Xu, T. Zhang, Y. Liu, D. Yang, L. Xiao, and M. Tao, "UAV-Assisted MEC Networks With Aerial and Ground Cooperation," *IEEE Transactions on Wireless Communications*, vol. 20, no. 12, pp. 7712–7727, Dec. 2021, doi: 10.1109/TWC.2021.3086521.

[3] H. Rahmani, G. Mirjalily, and J. Abouei, "Energy-Efficient Joint Resource Management and Trajectory Planning in UAV-Assisted NOMA-Based Mobile Edge Computing Networks," *IET Communications*, vol. 19, no. 1, 2025.

[4] Z. Sun, G. Sun, Q. Wu, L. He, S. Liang, H. Pan, D. Niyato, C. Yuen, and V. C. M. Leung, "TJCCT: A Two-Timescale Approach for UAV-Assisted Mobile Edge Computing," *IEEE Transactions on Mobile Computing*, 2024, doi: 10.1109/TMC.2024.3505155.

[5] S. Alhelaly, A. Muthanna, and I. A. Elgendy, "Optimizing Task Offloading Energy in Multi-User Multi-UAV-Enabled Mobile Edge-Cloud Computing Systems," *Applied Sciences*, vol. 12, p. 6566, 2022.

[6] Q. Tang, X. Qu, J. Wang, and S. He, “A Multi-UAV Assisted Non-Orthogonal Multiple Access Based Relay System for Minimal Receiving Rate Maximization,” *Research Square*, 2023, doi: 10.21203/rs.3.rs-2558446/v1.

[7] Z. Ding, D. Xu, R. Schober, and H. V. Poor, “Hybrid NOMA Offloading in Multi-User MEC Networks,” *IEEE Transactions on Wireless Communications*, vol. 21, no. 7, pp. 5377–5391, 2022.

[8] X. Zheng, M. Tahir, K. Aurangzeb, M. S. Anwar, M. Aamir, A. Farzan, and R. Ullah, “Non-Orthogonal Multiple Access-Based MEC for Energy-Efficient Task Offloading in E-Commerce Systems,” *Journal of Cloud Computing*, 2024.

[9] J. Xia, Y. Liu, and L. Tan, “Joint Optimization of Trajectory and Task Offloading for Cellular-Connected Multi-UAV Mobile Edge Computing,” *Chinese Journal of Electronics*, vol. 33, no. 2, 2024.

[10] J. Ji, K. Zhu, C. Yi, and D. Niyato, “Energy Consumption Minimization in UAV-Assisted Mobile-Edge Computing Systems: Joint Resource Allocation and Trajectory Design,” *IEEE Internet of Things Journal*, vol. 8, pp. 8570–8584, 2021.

[11] Z. Y. Yang, S. Z. Bi, and Y. J. A. Zhang, “Dynamic Trajectory and Offloading Control of UAV-Enabled MEC under User Mobility,” in *Proc. IEEE International Conference on Communications Workshops (ICC Workshops)*, Montreal, QC, Canada, pp. 1–6, 2021.

[12] Y. Liu, S. L. Xie, and Y. Zhang, “Cooperative Offloading and Resource Management for UAV-Enabled Mobile Edge Computing in Power IoT Systems,” *IEEE Transactions on Vehicular Technology*, vol. 69, no. 10, pp. 12229–12239, 2020.

[13] M. Li, N. Cheng, J. Gao, Y. Wang, and L. Zhao, “Energy-Efficient UAV-Assisted Mobile Edge Computing: Resource Allocation and Trajectory Optimization,” *IEEE Transactions on Vehicular Technology*, vol. 69, no. 3, 2020.

[14] Z. Wang, G. Wang, and S. Huang, “Energy-Efficient Mobile Edge Computing Assisted by Layered UAVs Based on Convex Optimization,” *Physical Communication*, vol. 65, p. 102382, Aug. 2024, doi: 10.1016/j.phycom.2024.102382.

[15] N. N. Ei, M. Alsenwi, Y. K. Tun, Z. Han, and C. S. Hong, “Energy-Efficient Resource Allocation in Multi-UAV-Assisted Two-Stage Edge Computing for Beyond 5G Networks,” *IEEE Transactions on Intelligent Transportation Systems*, vol. 23, no. 9, pp. 16421–16432, 2022.

[16] X. Zhang, J. Zhang, J. Xiong, L. Zhou, and J. Wei, “Energy-Efficient Multi-UAV-Enabled Multi-Access Edge Computing Incorporating NOMA,” *IEEE Internet of Things Journal*, vol. 7, no. 6, pp. 5613–5627, Jun. 2020, doi: 10.1109/JIOT.2020.2980035.

[17] Z. Liu, J. Qi, Y. Shen, K. Ma, and X. Guan, “Maximizing Energy Efficiency in UAV-Assisted NOMA–MEC Networks,” *IEEE Access*, vol. 10, pp. 24839–24854, 2022.

[18] Y. Liu, S. Zhang, X. Mu, Z. Ding, R. Schober, N. Al-Dhahir, E. Hossain, and X. Shen, “Evolution of NOMA Toward Next-Generation Multiple Access (NGMA) for 6G,” *IEEE Journal on Selected Areas in Communications*, vol. 40, no. 4, pp. 1037–1071, Apr. 2022.

[19] J. Peng, W. Tang, and H. Zhang, “Directional Antennas Modeling and Coverage Analysis of UAV-Assisted Networks,” *IEEE Wireless Communications Letters*, vol. 11, no. 10, pp. 2175–2179, Oct. 2022, doi: 10.1109/LWC.2022.3196227.

[20] J. Zhang, L. Zhou, F. Zhou, B. C. Seet, H. Zhang, Z. Cai, and J. Wei, “Computation-Efficient Offloading and Trajectory Scheduling for Multi-UAV-Assisted Mobile Edge Computing,” *IEEE Transactions on Vehicular Technology*, vol. 69, no. 2, pp. 2114–2125, Feb. 2020.

[21] F. Zhou, Y. Wu, H. Sun, and Z. Chu, “UAV-Enabled Mobile Edge Computing: Offloading Optimization and Trajectory Design,” in *Proc. IEEE International Conference on Communications (ICC)*, pp. 1–6, May 2018.

[22] B. Li and J. Chen, “Radio Map Assisted Approach for Interference-Aware Predictive UAV Communications,” *arXiv preprint arXiv:2402.00569*, Feb. 2024.

[23] M. Grant and S. Boyd, “CVX: MATLAB Software for Disciplined Convex Programming,” 2016. [Online]. Available: CVX Research official website

[24] Y. Zeng and R. Zhang, “Energy-Efficient UAV Communication with Trajectory Optimization,” *IEEE Transactions on Wireless Communications*, vol. 16, no. 6, Jun. 2017.